TABLE DR1. SUMMARY OF AVERAGE MAJOR AND TRACE ELEMENT COMPOSITIONS OF ZIRCON PHENOCRYSTS

| Element | % Uncertainty | | Analcite tuff (SB-1) | | | Firehole tuff (FC-2) | | |
|---|---|---|---|---|---|---|---|---|
| $SiO_2$ | 0.2 | | 32.8 | 32.8 | 32.7 | 33.2 | 31.8 | 33.3 |
| $ZrO_2$ | 0.6 | | 65.7 | 64.6 | 64.1 | 66.0 | 64.3 | 65.4 |
| $HfO_2$ | 0.6 | | 1.60 | 1.44 | 1.42 | 1.33 | 1.09 | 1.14 |
| Oxide Totals | | | 100.9 | 100.4 | 99.3 | 100.6 | 99.1 | 99.4 |
| ppm | | detection limit (99% confidence) | | | | | | |
| Y | 0.9 | 110 | 2757 | 5820 | 5293 | 3202 | 7442 | 1844 |
| Th | 8.4 | 390 | 2102 | 1583 | 853 | 1094 | 756 | bd |
| U | 1.5 | 400 | 3032 | 2302 | 1708 | 2213 | 1234 | 653 |
| P | 2.4 | 80 | 327 | 242 | 253 | 462 | 2253 | 685 |
| Yb | 4.3 | 410 | 1023 | 1467 | 1290 | 1060 | 2208 | 505 |

*Note:* bd indicates below detection limit

TABLE DR2. RECALIBRATED $^{40}Ar/^{39}Ar$ AGES FOR ASH BEDS IN THE GREEN RIVER FORMATION AND RELATED STRATA

| Name (sample) formation (abbr.) | | location | MSWD | Weighted Mean Age (Ma) ± 2σ[†§] | ±2σ[#] | ±2σ[††] |
|---|---|---|---|---|---|---|
| mineral | Analysis type | n | | | | |
| ***Greater Green River Basin*** | | | | | | |
| **Sage Creek Mt. pumice (SCM) Tb** | | N 41° 7' 56.5" W 110° 8' 11.7" | | | | |
| sanidine | SF + MI | 45 of 45 | 0.69 | **47.45 ± 0.08[‡]** | ± 0.12 | ± 0.15 |
| **Tabernacle Butte tuff (TaB) Tb** | | N 42° 26' 11.7" W 109° 22' 23.8" | | | | |
| sanidine | SF + MI | 40 of 40 | 0.78 | **48.40 ± 0.08[‡]** | ± 0.13 | ± 0.15 |
| **Henrys Fork tuff (HeF) Tb** | | N 41° 07' 25.3" W 110° 09' 27.7" | | | | |
| sanidine | SF + MF | 71 of 71 | 1.04 | **48.44 ± 0.08[‡]** | ± 0.13 | ± 0.15 |
| **Leavitt Creek tuff (LeC) Tb** | | N 41° 14' 13.1" W 110° 12' 41.8" | | | | |
| sanidine | SF | 12 of 14 | 0.28 | **48.92 ± 0.28[‡]** | ± 0.30 | ± 0.31 |
| **Church Buttes tuff (ChB) Tb** | | N 41° 28' 34.5" W 110° 08' 04.3" | | | | |
| sanidine | SF + MI | 42 of 46 | 1.30 | **49.05 ± 0.09[‡]** | ± 0.13 | ± 0.16 |
| **Continental Peak tuff (CP-1) Tb** | | N 42° 16' 06.2" W 108° 43' 7.5" | | | | |
| sanidine | MF | 12 of 16 | 0.29 | **48.96 ± 0.28[‡]** | ± 0.30 | ± 0.31 |
| **Analcite tuff (SB-1) Tgl** | | N 41° 21' 01.4" W 108° 40' 4.7" | | | | |
| sanidine | SF + MF | 30 of 40 | 0.59 | **49.24 ± 0.12[‡]** | ± 0.15 | ± 0.18 |
| **Sixth tuff (TR-5) Tgw** | | N 41° 32' 31.1" W 109° 28' 52.9" | | | | |
| sanidine | SF + MF | 45 of 70 | 0.13 | 49.96 ± 0.47 | ± 0.48 | ± 0.49 |
| biotite | SI + MI (21 of 26)[§§] | 119 of 142 | 1.00 | **49.92 ± 0.10[‡]** | ± 0.14 | ± 0.17 |
| **Layered tuff (TR-6) Tgw** | | N 41° 32' 33.6" W 109° 28' 55.6" | | | | |
| sanidine | MF[§§] | 64 of 73 | 0.42 | **50.11 ± 0.09[‡]** | ± 0.14 | ± 0.16 |
| **Main tuff (TR-1) Tgw** | | N 41° 32' 28.1" W 109° 28' 52.0" | | | | |
| sanidine | MF[‡‡] | 23 of 31 | 0.51 | **50.27 ± 0.09[‡]** | ± 0.13 | ± 0.16 |
| **Grey tuff (WN-1) Tgw** | | N 41° 39' 24.3" W 109° 17' 18.8" | | | | |
| sanidine | MF[‡‡] | 8 of 18 | 0.53 | **50.86 ± 0.21[‡]** | ± 0.23 | ± 0.25 |
| **Boar tuff (BT-14) Tgw** | | N 41° 57' 48.6" W 109° 15' 9.8" | | | | |
| sanidine | MF | 13 of 14[##] | 1.74 | **51.13 ± 0.24[‡]** | ± 0.26 | ± 0.27 |
| **Firehole tuff (FC-2) Tgw** | | N 41° 21' 00.7" W 109° 22' 59.9" | | | | |
| sanidine | MF | 20 of 41 | 0.36 | **51.40 ± 0.21[‡]** | ± 0.23 | ± 0.25 |
| **Rife tuff (BT-18) Tgt** | | N 41° 57' 47.2" W 109° 15' 8.7" | | | | |
| biotite | MF + SF[‡‡] | 15 of 38 | 0.68 | **51.61 ± 0.30[‡]** | ± 0.32 | ± 0.33 |
| **Scheggs tuff (WP-3) Tgt** | | N 41° 31' 09.9" W 109° 19' 29.8" | | | | |
| sanidine | SF + MF | 83 of 83 | 0.34 | **52.21 ± 0.09[‡]** | ± 0.14 | ± 0.16 |
| ***Fossil-Fowkes Basin*** | | | | | | |
| **K-spar tuff (FQ-1) Tgf** | | N 41° 47' 32.2" W 110° 42' 39.6" | | | | |
| sanidine | MF | 55 of 56 | 0.44 | **51.97 ± 0.09[‡]** | ± 0.14 | ± 0.16 |
| **Sage tuff (FF) Tf** | | N 41° 46' 44.8" W 110° 57' 50.4" | | | | |
| sanidine | MF | 18 of 25 | 0.43 | **48.23 ± 0.17[‡]** | ± 0.20 | ± 0.22 |

TABLE DR2. RECALIBRATED $^{40}Ar/^{39}Ar$ AGES FOR ASH BEDS IN THE GREEN RIVER FORMATION AND RELATED STRATA

| Name (sample) formation (abbr.) | | location | MSWD | Weighted Mean Age (Ma) ± 2σ[†§] | ±2σ[#] | ±2σ[††] |
|---|---|---|---|---|---|---|
| mineral | Analysis type | n | | | | |
| ***Piceance Creek Basin*** | | | | | | |
| **Yellow tuff (WR-1) Tgp** | | N 40º 01' 01.9" W 108º 6' 53.2" | | | | |
| sanidine | MF | 23 of 53 | 0.40 | **51.55 ± 0.52[‡]** | ± 0.53 | ± 0.54 |
| ***Uinta Basin*** | | | | | | |
| **Strawberry tuff (SR-1) Tgsl** | | N 40º 09' 54.0" W 110º 33' 5.6" | | | | |
| sanidine | SF + MF | 22 of 68 | 0.14 | **44.27 ± 0.93[‡]** | ± 0.93 | ± 0.93 |
| **Oily tuff (IC-6) Tgs** | | N 40º 02' 56.8" W 110º 31' 42.1" | | | | |
| biotite | SI (9 of 10) | 43 of 49 | 0.93 | **45.41 ± 0.10[‡]** | ± 0.14 | ± 0.16 |
| **Portly tuff (IC-5) Tgs** | | N 39º 58' 46.5" W 110º 37' 6.9" | | | | |
| biotite | SI + MI | 84 of 84 | 0.17 | **45.85 ± 0.14[‡]** | ± 0.17 | ± 0.19 |
| **Fat tuff (IC-2) Tgs** | | N 39º 58' 46.5" W 110º 37' 6.9" | | | | |
| biotite | SI (4 of 13) | 19 of 65 | 2.10 | **46.62 ± 0.13[‡]** | ± 0.16 | ± 0.18 |
| **Blind Canyon tuff (SW-1) Tgu** | | N 39º 50' 41.4" W 110º 11' 11.8" | | | | |
| biotite | SI + MI (3 of 13) | 13 of 73 | 0.10 | **47.32 ± 0.18[‡]** | ± 0.20 | ± 0.22 |
| **Wavy tuff (GC-2b) Tgu** | | N 39º 50' 59.3" W 110º 15' 17.5" | | | | |
| biotite | SI (4 of 18) | 23 of 107 | 0.51 | **48.66 ± 0.23[‡]** | ± 0.25 | ± 0.27 |
| **Curly tuff (GC-5b) Tgu** | | N 39º 50' 33.8" W 110º 15' 3.1" | | | | |
| biotite | SI (4 of 10) | 11 of 26 | 0.68 | **49.32 ± 0.30[‡]** | ± 0.32 | ± 0.33 |
| ***Wind River Basin*** | | | | | | |
| **White Lignitic tuff (WB-1) Twb** | | N 42º 42' 54.3" W 108º 11' 11.8" | | | | |
| sanidine | SF + MF | 34 of 36 | 1.02 | **47.99 ± 0.12[‡]** | ± 0.15 | ± 0.17 |
| **Halfway Draw tuff (HD-1) Twr** | | N 42º 51' 51.0" W 108º 11' 58.1" | | | | |
| sanidine | SF + MI | 60 of 73 | 0.41 | **52.06 ± 0.10[‡]** | ± 0.14 | ± 0.17 |

*Notes*: *Notes:* All ages recalculated from Smith et al. (2008) unless otherwise noted. Twi–Willwood Formation, Twr–Wind River Formation, Twb–Wagon Bed Formation, Tb–Bridger Formation, Tgl–Laney Member-Green River Formation, Tgw–Wilkins Peak Member-Green River Formation, Tgt–Tipton Member-Green River Formation, Tgf–Fossil Butte Member-Green River Formation, Tf–Fowkes Formation, Tgsl–sandstone and limestone member-Green River Formation, Tgs–saline member-Green River Formation, Tgp–Parachute Creek Member-Green River Formation. All sanidine analyses yielding less that 96% $^{40}Ar^*$ have been excluded from weighted mean age calculations. Only experiments yielding 100% concordant age spectra are included in calculation of weighted means of plateau ages. MI–multicrystal laser incremental heating experiments, SI–single crystal laser incremental heating experiments, MF–multicrystal laser fusion experiments, SF–single crystal laser fusion experiments, IA–integrated ages. Concordant experiments include all incremental heating steps. MSWD–mean square weighted deviate. Latitude and longitude referenced to NAD27 datum.

[†]Ages reported relative to 28.201 Ma for FCs (Kuiper et al., 2008) and intercalibration values (R) of Renne et al. (1998).

[‡]**Preferred age**

[§]Analytical uncertainty

[#]Analytical and intercalibration uncertainty, calculated using R values of Renne et al. (1998)

[††]Fully propagated uncertainty for preferred age from equations in Kuiper et al. (2008)

[‡‡]From Smith et al. (2003)

[§§]From Smith et al. (2006)

[##]Three previously excluded analyses (UW11G1a, h, and l; Smith et al., 2008) included in revised weighted mean age.

## TABLE DR3. COMPLETE U-Pb RESULTS

| Sample<br>analysis | n | Mass (µg) | U (ppm) | $Pb_s$[§] (ppm) | (pg) | $Pb_i$[#] (ppm) | (pg) | $Pb^*$[‡]/$Pb_c$[†] | $^{206}Pb$[‡]/$^{204}Pb$ | Corrected atomic ratios** $^{206}Pb/^{204}Pb$ | $^{206}Pb/^{208}Pb$ | $^{206}Pb/^{238}U$ Ratio ± 2σ (%) | $^{207}Pb/^{235}U$ Ratio ± 2σ (%) | $^{207}Pb/^{206}Pb$ Ratio ± 2σ (%) | $^{206}Pb/^{238}U$ Age (Ma) | $^{206}Pb/^{238}U$ Age[††] (Ma) ± 2σ | $^{207}Pb/^{235}U$ Age (Ma) ± 2σ | $^{207}Pb/^{206}Pb$ Age (Ma) | σ[§§] |
|---|---|---|---|---|---|---|---|---|---|---|---|---|---|---|---|---|---|---|---|
| **Firehole tuff (FC-2) N41°21'0.7" W109°22'59.9" [##]** | | | | | | | | | | | | | | | | | | | |
| ls pE C | 3 | 2.6 | 269 | 2.38 | 6 | 0.15 | 0.4 | 1.8 | 120 | 996 | 11.1 | 0.008477 ± 0.65 | 0.05653 ± 5.01 | 0.0484 ± 4.67 | 54.42 | 54.51 ± 0.35 | 55.83 ± 2.72 | 117 | 0.57 |
| nm4 a p2 | 10 | 13.9 | 377 | 3.40 | 47 | 0.13 | 1.9 | 9.7 | 506 | 1527 | 6.05 | 0.008315 ± 0.36 | 0.05559 ± 0.92 | 0.0485 ± 0.80 | 53.38 | 53.47 ± 0.19 | 54.93 ± 0.49 | 123 | 0.51 |
| ***nm10 C st4*** | 120[§] | 237 | 113 | 1.03 | 244 | 0.11 | 26.8 | 8.2 | 347 | 539 | 8.76 | 0.008103 ± 0.32 | 0.05283 ± 0.67 | 0.0473 ± 0.55 | 52.02 | ***52.12 ± 0.17*** | 52.27 ± 0.34 | 64 | 0.58 |
| ***tip p2 C E*** | 6 | 3.3 | 127 | 1.01 | 3 | 0.00 | 0.0 | 1.1 | 83 | 40141 | 11.0 | 0.008094 ± 1.65 | 0.05396 ± 19.3 | 0.0484 ± 17.8 | 51.97 | ***52.06 ± 0.85*** | 53.36 ± 10.0 | 129 | 0.89 |
| ***tip p4 a C E*** | 10 | 14.9 | 274 | 2.38 | 35 | 0.20 | 3.0 | 5.5 | 345 | 733 | 9.85 | 0.008050 ± 0.19 | 0.05253 ± 2.13 | 0.0473 ± 1.97 | 51.69 | ***51.78 ± 0.10*** | 51.98 ± 1.08 | 66 | 0.86 |
| ***eq pk1 C E*** | 5 | 4.7 | 159 | 1.41 | 7 | 0.17 | 0.8 | 1.8 | 109 | 527 | 11.0 | 0.008036 ± 0.99 | 0.05139 ± 12.1 | 0.0464 ± 11.3 | 51.60 | ***51.69 ± 0.51*** | 50.89 ± 6.02 | 25 | 0.86 |
| ***syn p6 C E*** | 6 | 36.3 | 205 | 1.74 | 63 | 0.11 | 3.8 | 8.6 | 543 | 1027 | 9.00 | 0.008022 ± 0.11 | 0.05259 ± 1.17 | 0.0476 ± 1.09 | 51.51 | ***51.60 ± 0.06*** | 52.04 ± 0.60 | 77 | 0.82 |
| ***ls pC C*** | 3 | 3.9 | 1336 | 12.51 | 49 | 2.05 | 8.0 | 4.4 | 249 | 353 | 10.6 | 0.007977 ± 0.36 | 0.05183 ± 0.92 | 0.0471 ± 0.81 | 51.22 | ***51.32 ± 0.19*** | 51.31 ± 0.46 | 55 | 0.50 |
| ls pA C | 3 | 4.2 | 260 | 2.04 | 9 | 0.03 | 0.1 | 2.7 | 176 | 4112 | 8.81 | 0.007731 ± 0.69 | 0.05094 ± 2.88 | 0.0478 ± 2.61 | 49.64 | 49.74 ± 0.34 | 50.45 ± 1.42 | 89 | 0.50 |
| ***Weighted mean of $^{230}Th$ disequilibrium-corrected $^{206}Pb/^{238}U$ ages = 51.66 ± 0.19 Ma [0.37%] (±0.20 Ma w/decay and tracer error) MSWD = 11.2*** | | | | | | | | | | | | | | | | | | | |
| **Analcite tuff (SB-1) N41°21'1.4" W108°40'4.7" [##]** | | | | | | | | | | | | | | | | | | | |
| ***nm4 C st3*** | 86[§] | 306 | 172 | 1.41 | 430 | 0.02 | 6.0 | 47.9 | 1197 | 4247 | 5.95 | 0.007683 ± 0.32 | 0.04999 ± 0.44 | 0.0472 ± 0.27 | 49.34 | ***49.43 ± 0.16*** | 49.54 ± 0.21 | 59 | 0.79 |
| ***p1 C E*** | 3 | 10.6 | 2065 | 16.55 | 175 | 0.08 | 0.8 | 40.4 | 2495 | 12540 | 6.13 | 0.007657 ± 0.09 | 0.04974 ± 0.28 | 0.0471 ± 0.24 | 49.17 | **49.26 ± 0.05** | 49.29 ± 0.13 | 55 | 0.51 |
| ***nm4 C st4*** | 86[§] | 306 | 327 | 2.63 | 805 | 0.01 | 4.4 | 109 | 2483 | 10923 | 5.95 | 0.007656 ± 0.36 | 0.04996 ± 0.41 | 0.0473 ± 0.18 | 49.17 | ***49.25 ± 0.17*** | 49.50 ± 0.20 | 66 | 0.90 |
| ***nm2 p8 a*** | 11 | 8.4 | 610 | 5.08 | 42 | 0.17 | 1.4 | 9.6 | 471 | 1700 | 5.71 | 0.007649 ± 0.38 | 0.04996 ± 0.89 | 0.0474 ± 0.73 | 49.12 | ***49.21 ± 0.19*** | 49.50 ± 0.43 | 68 | 0.60 |
| ***nm4 C st2*** | 86[§] | 306 | 95 | 0.80 | 246 | 0.04 | 13.2 | 15.2 | 499 | 1065 | 5.75 | 0.007615 ± 0.37 | 0.04964 ± 0.68 | 0.0473 ± 0.52 | 48.91 | ***48.99 ± 0.18*** | 49.20 ± 0.33 | 63 | 0.66 |
| ***nm4 C st5*** | 86[§] | 306 | 369 | 3.20 | 978 | 0.26 | 79.3 | 11.9 | 585 | 693 | 5.93 | 0.007606 ± 0.36 | 0.04966 ± 0.47 | 0.0474 ± 0.28 | 48.85 | ***48.93 ± 0.18*** | 49.21 ± 0.22 | 67 | 0.80 |
| ***pC C*** | 3 | 7.4 | 276 | 2.26 | 17 | 0.09 | 0.6 | 4.6 | 218 | 1542 | 6.24 | 0.007570 ± 0.58 | 0.04862 ± 2.17 | 0.0466 ± 1.88 | 48.62 | ***48.70 ± 0.28*** | 48.21 ± 1.02 | 28 | 0.60 |
| pB C | 3 | 3.5 | 700 | 5.71 | 20 | 0.43 | 1.5 | 4.4 | 317 | 738 | 5.54 | 0.007145 ± 0.49 | 0.04638 ± 1.28 | 0.0471 ± 1.09 | 45.89 | 45.98 ± 0.22 | 46.04 ± 0.58 | 54 | 0.55 |
| ***Weighted mean of $^{230}Th$ disequilibrium-corrected $^{206}Pb/^{238}U$ ages = 49.23 ± 0.12 Ma [0.25%] (± 0.13 Ma w/decay and tracer error) MSWD = 6.7*** | | | | | | | | | | | | | | | | | | | |

*Radiogenic Pb.

[†]Total common Pb (blank + initial).

[§]Radiogenic + initial Pb, corrected for laboratory blank of 3 pg. Note that U and Pb concentrations are based on initial mass and that chemically abraded analyses give underestimations because only a portion of the aliquot was removed in the successive chemical leaching steps.

[#]Common Pb corrected for laboratory blank of 3 pg Pb. Isotopic composition of blank = 18.719 ± 0.97 ($^{206}Pb/^{204}Pb$), 15.662 ± 0.57 ($^{207}Pb/^{204}Pb$), and 38.226 ± 1.42 ($^{208}Pb/^{204}Pb$). Isotopic compositions of initial Pb were based on co-existing feldspar Pb isotopic compositions ($^{206}Pb/^{204}Pb$ = 18.966 ± 0.021, $^{207}Pb/^{204}Pb$ = 15.634 ± 0.024, $^{208}Pb/^{204}Pb$ = 38.692 ± 0.080 for FC-2, 17.848 ± 0.018, 15.489 ± 0.023, 37.764±0.075 for SB-1, see Fig. DR1).

[‡]Measured, corrected for mass discrimination and tracer.

** $^{206}Pb/^{204}Pb$ corrected for blank, mass discrimination and tracer, all others corrected for blank, mass discrimination, tracer and initial Pb.

[††] Corrected for $^{230}Th$-disequilibrium using radiogenic $^{208}Pb/^{206}Pb$, radiogenic $^{206}Pb/^{238}U$ and an estimated magmatic Th/U of 2.85.

[§§] $^{206}Pb/^{238}U$ vs. $^{207}Pb/^{235}U$ error correlation coefficient.

[##]Geographic coordinates of sampling location given relative to the NAD1927 datum.

***Notes*** Samples in bold italics are included in weighted means. n: number of grains or fragments dissolved. Mass: mass prior to first step of either CA-TIMS or total dissolution. Mineral dissolution and chemistry were adapted from methods developed by Krogh (1973), Parrish et al. (1987) and Mattinson (2005). 15 of 17 zircon fractions were dissolved in steps using the CA-TIMS method (Mattinson 2005). The chemically abraded grains were first annealed at 850 °C for 48 hours, then dissolved in HF and $HNO_3$ in either multiple steps, closely following Mattinson (2005), or in a modified two-step process. In both

cases, the solutions from the first dissolution step were discarded and only the data from the later steps were used for geochronology. Mechanically abraded grains that were not also chemically abraded were dissolved in a single step with HF and $HNO_3$ at 240 °C for 30 hours. Analysis name convention: nm_=paramagnetic split on isodynamic separator; a=mechanically abraded; C=chemically abraded; st_=step in multi-step dissolution; ls=long slender euhedral grains; eq=equant euhedral grains; tip=tips of grains; syn=synneusis twinned grains; p_ =pick identifier; E=spiked with mixed $^{205}Pb$ spike ET535. Isotope dilutions were from either a mixed $^{208}Pb/^{235}U$ tracer added to an aliquot of the final dissolution or from $^{205}Pb/^{233}U/^{235}U$ tracer (ET535) added to the total. Pb and U samples were purified on HCl ion exchange columns modified from Krogh (1973), and loaded onto single rhenium filaments with silica gel and graphite, respectively; isotopic compositions were measured in either single Daly mode or multi- collector, static mode on a Micromass Sector 54 mass spectrometer at the University of Wyoming with $^{204}Pb$ in Daly-photomultiplier collector and all other isotopes in Faraday collectors. Mass discrimination for Pb of 0.060 ± 0.06 %/amu for static Faraday runs and 0.185 ± 0.06%/amu for single Daly runs were determined by replicate analyses of NIST SRM 981. U fractionation was 0.0 ± 0.06%/amu based on replicate analyses of NIST U500, or determined internally during each run using the ET535 spike. Procedural blanks averaged 3 pg Pb for zircon during the course of the study. Isotopic composition of the Pb blank was measured as 18.719±0.97, 15.662±0.57, and 38.226±1.42 for $^{206}Pb/^{204}Pb$, $^{207}Pb/^{204}Pb$ and $^{208}Pb/^{204}Pb$, respectively. U blanks were consistently less than 0.2 pg. Concordia coordinates, intercepts, and uncertainties were calculated using MacPBDAT and ISOPLOT programs (based on Ludwig 1988, 1991); initial Pb isotopic compositions were estimated from Pb isotopic compositions of co-existing feldspar. The decay constants used by MacPBDAT are those recommended by the I.U.G.S. Subcommission on Geochronology (Steiger and Jäger, 1977): $0.155125 \times 10^{-9}$/yr for $^{238}U$, $0.98485 \times 10^{-9}$/yr for $^{235}U$ and present-day $^{238}U/^{235}U = 137.88$. $^{208}Pb/^{235}U$ tracer was calibrated against MIT2 gravimetric standard and yielded a $^{206}Pb/^{238}U$ date of 419.26 ± 0.64 Ma for zircon standard R33 ($^{207}Pb/^{235}U$ date of 420.11 ± 0.59 Ma), in good agreement with the ROM date for R33 (Black et al., 2004).

***Common Pb corrections**:* Previous analyses of mechanically abraded zircons from these ashes had established unusually high amounts of common Pb (10 to 15 ppm, 30 to 100 picograms and up to 75% of the total sample Pb (Smith, 2007)). Neither the blank isotopic compositions nor those of co-existing feldspars adequately matched the isotopic compositions of the common Pb in these previous analyses. The source of the Pb was interpreted to be labile Pb introduced into the crystal structure during diagenesis in the alkaline lake environment (Smith, 2007). Fortunately, the chemical abrasion method of Mattinson (2005) removes most of this labile common Pb, and chemical abrasion methods were used for most of the analyses reported in this paper. To minimize the effects of common Pb corrections and the uncertainties associated with its isotopic composition, only analyses with blank-corrected $^{206}Pb/^{204}Pb$ greater than 300 are reported here and used for geochronologic interpretations. The Pb isotopic compositions of sanidine from FC-2 overlap with those of the blank composition at UW, so partitioning of common Pb between blank and initial Pb has negligible effect on the calculated radiogenic values from this sample. The proportions of radiogenic to total common Pb for most of the analyses from SB-1 are high enough that blank vs. initial partitioning has little effect here as well, even though the sanidine values are distinct from UW blank compositions.

***$^{230}$Th disequilibrium correction:*** Magmatic partitioning of relatively long-lived intermediate daughter products of the U-Pb decay chain in zircon crystals can lead to measurable systematic inaccuracy in U-Pb ages (Schärer, 1984). The most significant mineralogic partitioning for samples older than ~15 Ma is a preference for U versus Th in zircon that leads to a deficiency in $^{230}Th$, which in turn leads to systematically underestimated $^{238}U/^{206}Pb$ ages (Schmitz and Bowring, 2001). Ideally, the degree to which $^{230}Th$ disequilibrium affects $^{206}Pb/^{238}U$ age can be accounted for by measuring the magmatic U/Th ratio using primary volcanic glass. Unfortunately, there is no unaltered glass remaining in the sampled ash beds due to its conversion to zeolite minerals by reactions with alkaline lake waters (Surdam and Parker, 1972). Consequently, we used the equations of Schärer (1984) to model the magnitude of potential systematic age offset due to $^{230}Th$ disequilibrium for 50 Ma zircons (c.f. Schmitz and Bowring, 2001). Modeled correction values for the Analcite and Firehole tuff zircon analyses range from +0.75% to +0.85% (+0.09 to +0.10 Myr), and are relatively insensitive to different magma compositions at ~50 Ma, varying by only ± 4000 years (< 0.01%) when relatively end member Th/U values of 2.1 and 4 are considered. We have therefore selected an arbitrary value of 2.85 for magmatic Th/U for use in all $^{230}Th$ disequilibrium corrected age calculations reported in this paper.

Table DR4. RECALIBRATED $^{40}Ar/^{39}Ar$ AGES FOR EOCENE STRATA, IGNEOUS ROCKS, AND METAMORPHIC CORE COMPLEXES OF THE NORTHERN ROCKY MOUNTAINS

| *Location* Sample | Stratigraphy | Dated Material | Method | flux monitor | Age* (Ma) | ± 2σ† | ± 2σ‡ | ± 2σ§ | References |
|---|---|---|---|---|---|---|---|---|---|
| *Plateau province* | | | | | | | | | |
| ET-8 | Tg | bio & hbd | ih | Mmhb | 43.96 | 1.30 | 1.30 | 1.30 | Sheliga (1980) |
| ST-2 | Tg | feld | ih | | 47.01 | 2.27 | 2.27 | 2.27 | |
| WCT-1 | Tg | bio | ih | | 44.21 | 0.99 | 0.99 | 1.00 | |
| *Uinta Basin* | | | | | | | | | |
| Sample 14 | Tg | bio | ? | ? | 45.61 | 0.34 | 0.34 | 0.36 | Constenius et al. (2003) |
| *Bighorn Basin* | | | | | | | | | |
| Willwood Ash | Twi | san | combo | TCs | 52.90 | 0.12 | 0.16 | 0.18 | Smith et al. (2004) |
| *Absaroka Volcanic Province-Intrusions* | | | | | | | | | |
| AR76-121 | Dunrud Pk rhyolite | san | dih | FCs | 44.24 | 0.18 | 0.18 | 0.20 | Hiza (1999) |
| AR76-120 | Kirwin dacite (Mt Burwell) | hbld | dih | | 45.39 | 1.72 | 1.72 | 1.72 | |
| AR77-184 | Rampart banackite | bio | ih | | 47.15 | 0.22 | 0.22 | 0.24 | |
| 70-0-4 | Ishawooa banackite | bio | ih | | 47.57 | 0.18 | 0.18 | 0.20 | |
| HMD4-96 | Sunlight (White Mt) monzogabbro | bio | dih | | 48.83 | 0.16 | 0.16 | 0.18 | |
| HM1-94 | Crandall banakite | hbld | ih | | 49.75 | 0.18 | 0.18 | 0.20 | |
| YFP7-93 | S. Gallatin Range dacite | bio | ih | | 50.64 | 0.18 | 0.18 | 0.20 | |
| PR2-93 | Golmeyer Cr andesite dike | bio | dih | | 52.22 | 0.41 | 0.41 | 0.41 | |
| YGDC1-96 | Bighorn Peak dacite | hbld | | | 54.33 | 0.61 | 0.61 | 0.61 | |
| *Absaroka Volcanic Province-Extrusive* | | | | | | | | | |
| 70-0-13 | Pinnacle Butte ash | san | ih | | 47.57 | 0.18 | 0.18 | 0.20 | |
| 68-0-51 | Blue point ash (Irish Rock) | hbld | ih | | 48.31 | 0.20 | 0.20 | 0.22 | |
| 3497 | Blue point ash (Two Ocean) | feld | ih | | 48.41 | 0.14 | 0.14 | 0.17 | |
| P-348 | Lost Creek tuff | san | ih | | 49.40 | 0.16 | 0.16 | 0.18 | |
| P-306 | Pacific Creek tuff | bio | ih | | 49.52 | 0.24 | 0.24 | 0.26 | |
| YCS-5-95 | Slough Creek tuff Aslan Member | san | ih | | 50.25 | 0.16 | 0.16 | 0.18 | |
| YCS-3-95 | Slough Creek tuff upper rhyolitic unit | bio | dih | | 50.43 | 0.20 | 0.20 | 0.22 | |
| HHM17B-95 | Crandall trachyte ash-flow tuff | bio | ih | | 50.65 | 0.28 | 0.28 | 0.30 | |
| YRL1-93 | Sepulcher Mtn ash-flow | bio | dih | | 54.04 | 0.61 | 0.61 | 0.61 | |
| *Independence Volcano* | | | | | | | | | |
| 2085 | Independence stock | bio | ih | Mmhb | 49.09 | 0.12 | 0.13 | 0.15 | Harlan et al. (1996) |
| 1054 | " | " | ih | | 49.12 | 0.12 | 0.13 | 0.15 | |
| IN8 | " | " | ih | | 49.22 | 0.15 | 0.16 | 0.18 | |
| 2117 | " | " | ih | | 49.68 | 0.11 | 0.12 | 0.15 | |
| 1077 | dacite sill | bio | ih | | 50.57 | 0.17 | 0.18 | 0.20 | |
| 91IN2 | basal dacite breccia above Paleozoic | hbld | ih | | 52.16 | 0.14 | 0.15 | 0.17 | |
| *Washburn Volcano* | | | | | | | | | |
| MW9743 | andesite | gm | ih iso | Mmhb | 52.53 | 0.81 | 0.81 | 0.82 | Feeley et al. (2002) |
| MW9746 | sulphur creek stock | bio | ih iso | | 53.24 | 0.20 | 0.21 | 0.22 | |
| MW97-01 | dacitic lava flow at base of sequence | gm | ih iso | | 55.87 | 0.61 | 0.61 | 0.62 | |

Table DR4. RECALIBRATED $^{40}Ar/^{39}Ar$ AGES FOR EOCENE STRATA, IGNEOUS ROCKS, AND METAMORPHIC CORE COMPLEXES OF THE NORTHERN ROCKY MOUNTAINS

| *Location* Sample | Stratigraphy | Dated Material | Method | flux monitor | Age* (Ma) | ± 2σ† | ± 2σ‡ | ± 2σ§ | References |
|---|---|---|---|---|---|---|---|---|---|
| *Sunlight Volcano* | | | | | | | | | |
| SV97-02 | upper Trout Peak Trachyandesite | gm | ih | Mmhb | 48.69 | 0.10 | 0.11 | 0.14 | Feeley and Cosca (2003) |
| SV97-37 | trachytic core of Copper Lakes stock | bio | ih | | 48.73 | 0.08 | 0.09 | 0.13 | |
| SV97-07 | base of Trout Peak Trachyandesite | gm | ih | | 48.94 | 0.10 | 0.11 | 0.14 | |
| SV97-14 | top of lower Trout Peak Trachyandesite | gm | ih | | 49.08 | 0.10 | 0.11 | 0.14 | |
| SV97-33 | trachyte dike on Black Mtn | bio | ih | | 49.80 | 0.10 | 0.11 | 0.14 | |
| SV97-03 | base of Jim Mountain Mb. of Wapiti Fm. | plag | ih | | 50.10 | 0.16 | 0.17 | 0.19 | |
| SV97-29 | "Langford Fm." on Black Mtn. | amph | ih | | 50.15 | 0.16 | 0.17 | 0.19 | |
| *Crazy Mountains* | | | | | | | | | |
| diorite and gabbro | Big Timber Stock | bio | ? | Mmhb | 49.80 | 0.14 | 0.15 | 0.17 | S.S. Harlan, in Wilson and Elliot (1997) |
| | " | bio | ? | | 49.93 | 0.22 | 0.23 | 0.24 | |
| quartz monzodiorite | " | bio | ? | | 49.83 | 0.20 | 0.21 | 0.22 | |
| | " | bio | ? | | 49.93 | 0.24 | 0.25 | 0.24 | |
| *SE Challis Volcanics* | | | | | | | | | |
| DG-711-88 | porphyritic rhyolite intrusion (Trpi: Navarre Creek Dome) | bio | ih | Mmhb | 48.05 | 0.26 | 0.27 | 0.28 | Snider (1995) |
| | " | bio | ih | | 48.36 | 0.28 | 0.29 | 0.30 | |
| MD-620-88 | rhyolite dike (Trpi) | bio | ih | | 48.40 | 0.26 | 0.27 | 0.28 | |
| JDB-422-87 | rhyolite intrusion Porphyry Peak (Tri) | bio | ih | | 48.89 | 0.26 | 0.27 | 0.28 | |
| KK-345-89 | Garfield stock (Tg) | bio | dih | | 49.10 | 0.26 | 0.27 | 0.28 | |
| LS-369-89 | upper dacite flow/dome (Tdu) | bio | ih | | 47.89 | 0.26 | 0.27 | 0.28 | |
| LS-659-89 | tuff of Stoddard Gulch (Ts) | bio | ih | | 47.95 | 0.30 | 0.31 | 0.32 | |
| FJM-72B-87 | ryolite flow/dome complex at The Needles (Tru) | san | ih | | 48.02 | 0.32 | 0.33 | 0.34 | |
| LS-392-89 | lower rhyolite lavas (Tri) | bio | ih | | 48.69 | 0.57 | 0.57 | 0.57 | |
| JDB-462-87 | lower latite lavas (Tll) | bio | ih | | 49.39 | 0.34 | 0.35 | 0.36 | |
| LS-616c-87 | lower dacite flow/dome (Tdl) | bio | ih | | 49.45 | 0.49 | 0.49 | 0.50 | |
| Tdu/Tru | rhyolite flow | san | ih | Mmhb | 48.02 | 0.32 | 0.33 | 0.34 | Snider and Moye (1989) |
| Tll | tuff breccia | bio | ih | | 49.39 | 0.34 | 0.35 | 0.36 | |
| Tri | Boone Creek stock | bio | ih | | 49.45 | 0.26 | 0.27 | 0.28 | |
| Tch | tuff of Cherry Creek | san | ih | | 49.47 | 1.03 | 1.03 | 1.04 | |
| Tdl | tuff breccia | bio | ih | | 49.53 | 0.53 | 0.53 | 0.53 | |
| *E Challis Volcanics* | | | | | | | | | |
| 88-141 | tuff in Wet Creek cglm | san | ih | Mmhb | 45.95 | 0.20 | 0.21 | 0.22 | Janecke and Snee (1993) |
| 88-136 | Tuff of Challis Creek | san | ih | | 46.26 | 0.20 | 0.21 | 0.22 | |
| 88-100 | rhyolite tuff | san | ih | | 46.66 | 0.40 | 0.41 | 0.42 | |
| 88-134 | tuff of mud lake | bio | dih | | 48.28 | 0.40 | 0.41 | 0.42 | |
| 88-222 | tuff in andesite flows | hbld | ih | | 48.79 | 0.81 | 0.81 | 0.82 | |
| 88-138 | dacite of Warren Mt | hbld | ih | | 48.99 | 0.61 | 0.61 | 0.61 | |
| 88-146 | andesite lava flow | hbld | dih | | 49.09 | 0.20 | 0.21 | 0.22 | |
| 88-133 | dacite of Crow's Nest Canyon | hbld | ih | | 49.19 | 0.20 | 0.21 | 0.22 | |
| 88-139 | dacite of Warren Mt. | hbld | ih | | 49.39 | 0.40 | 0.41 | 0.42 | |
| 88-88 | tuff in andesite flows | bio | ih | | 49.60 | 0.40 | 0.41 | 0.42 | |
| 88-143 | dacite lava flow | hbld | ih | | 49.80 | 0.61 | 0.61 | 0.61 | |

Table DR4. RECALIBRATED $^{40}Ar/^{39}Ar$ AGES FOR EOCENE STRATA, IGNEOUS ROCKS, AND METAMORPHIC CORE COMPLEXES OF THE NORTHERN ROCKY MOUNTAINS

| *Location* Sample | Stratigraphy | Dated Material | Method | flux monitor | Age* (Ma) | ± 2σ† | ± 2σ‡ | ± 2σ§ | References |
|---|---|---|---|---|---|---|---|---|---|
| 8 (Tc 1) | vitric tuff above (5) Lehmi Pass, Beaverhead Mtns | san | fus | TCs | 48.96 | 0.24 | 0.26 | 0.28 | M'Gonigle and Dalrymple (1996) |
| 7 (88-100) | basal lithic tuff Tendoy Mtns | san | fus | | 49.21 | 0.35 | 0.36 | 0.37 | |
| 6 (87-64) | basal lithic tuff Tendoy Mtns | san | fus | | 49.63 | 0.37 | 0.38 | 0.39 | |
| 5 (Tcq) | basal rhyolite tuff Lehmi Pass, Beaverhead Mtns | san | fus | | 49.66 | 0.24 | 0.26 | 0.28 | |
| *Panther Creek Basin* | | | | | | | | | |
| 6-22-4 | Tck - Tuffs of Castle Rock | san | ih | Mmhb | 45.91 | 0.20 | 0.21 | 0.22 | Janecke et al. (1997) |
| 93-1 | Tuffs of Challis Creek | san | ih | | 46.26 | 0.16 | 0.17 | 0.19 | |
| 6-18-10 | Tvl1 -Fractured ash flow tuff | san | ih | | 46.29 | 0.20 | 0.21 | 0.22 | |
| *Horse Prairie Basin* | | | | | | | | | |
| 8 | aphanitic mafic lava flow overlying Bloody Dick fault | gm | ih | FCs | 48.12 | 0.85 | 0.85 | 0.86 | Vandenburg et al. (1998) |
| 5 | top of undivided Challis volcanics | san | fus | | 48.14 | 0.26 | 0.26 | 0.28 | |
| 7 | volcanic breccia within Ts1 | gm | dih | | 48.17 | 1.19 | 1.20 | 1.20 | |
| 4 | base of undivided Challis volcanics | san | fus | | 49.57 | 0.34 | 0.34 | 0.36 | |
| 3 | base of undivided Challis volcanics | san | fus | | 50.00 | 1.34 | 1.34 | 1.34 | |
| 13 (82-322) | rhyolitic ash-flow tuff, top of CVG | san | fus | TCs | 46.90 | 0.35 | 0.36 | 0.37 | M'Gonigle and Dalrymple (1996) |
| 11 (88-59) | rhyolitic welded ash-flow tuff in basal volcanics | san | fus | | 47.06 | 0.41 | 0.42 | 0.43 | |
| 3 (82-528) | basal crystal-lithic tuff | san | fus | | 49.79 | 0.35 | 0.36 | 0.37 | |
| *Muddy Creek Basin* | | | | | | | | | |
| 4 | 10 cm tephra in tuffaceous shale | san | fus | FCs | 45.75 | 0.45 | 0.45 | 0.45 | Janecke et al. (1999) |
| 2 | biotitic ash flow tuff in facies A | san | fus | | 47.67 | 0.53 | 0.53 | 0.53 | |
| 1 | quartzite bearing ash flow tuff - basal unit | san | fus | | 50.10 | 0.10 | 0.10 | 0.13 | |
| 9 (91-171) | crystal-lithic tuff base of tuffaceous facies | san | fus | TCs | 48.06 | 0.27 | 0.28 | 0.30 | M'Gonigle and Dalrymple (1996) |
| *Sage Creek Basin* | | | | | | | | | |
| 17 (91-170) | crystal tuff | san | fus | TCs | 46.50 | 0.22 | 0.24 | 0.26 | M'Gonigle and Dalrymple (1996) |
| *Medicine Lodge Basin* | | | | | | | | | |
| 18 (91-104) | lithic tuff, overlying Proterozoic | san | fus | TCs | 45.99 | 0.27 | 0.28 | 0.29 | M'Gonigle and Dalrymple (1996) |
| 16 (87-63) | rhyolitic welded ash-flow tuff overlies Archean | san | fus | | 46.66 | 0.29 | 0.30 | 0.31 | |
| 15 (89-135-4) | crystal-lithic tuff, overlies (10), base of lake deposits | san | fus | | 46.68 | 0.33 | 0.34 | 0.35 | |
| 14 (82-551) | crystal-lithic tuff, base of sediments | san | fus | | 46.76 | 0.29 | 0.30 | 0.31 | |
| 12 (81-189) | rhyolitic welded ash-flow tuff in ss above CVG beds | san | fus | | 47.01 | 0.31 | 0.32 | 0.33 | |
| 10 (89-135-3) | crystal-lithic tuff above 700 m andesite-basalt flows below (15) | san | fus | | 47.35 | 0.37 | 0.38 | 0.39 | |
| 4 (82-504) | basal rhyolite | san | fus | | 49.72 | 0.37 | 0.38 | 0.39 | |

Table DR4. RECALIBRATED $^{40}Ar/^{39}Ar$ AGES FOR EOCENE STRATA, IGNEOUS ROCKS, AND METAMORPHIC CORE COMPLEXES OF THE NORTHERN ROCKY MOUNTAINS

| *Location* Sample | Stratigraphy | Dated Material | Method | flux monitor | Age* (Ma) | ± 2σ† | ± 2σ‡ | ± 2σ§ | References |
|---|---|---|---|---|---|---|---|---|---|
| *Lowland Creek Volcanics* | | | | | | | | | |
| LVC-32 | intrusive rhyolite | san | ih | Mmhb | 49.11 | 0.49 | 0.49 | 0.50 | Ispolatov (1997) |
| LVC-15 | dacite porphyry | hbld | | | 50.38 | 0.47 | 0.47 | 0.48 | |
| LVC-18 | andesite porphyry | plag | | | 50.89 | 2.15 | 2.15 | 2.15 | |
| LVC-6 | rhyodacite porphyry clast in rhyolite tuff | bio | | | 52.12 | 0.41 | 0.41 | 0.42 | |
| 95LVC-9 | rhyodacite porphyry flow | hbld | | | 52.94 | 0.39 | 0.39 | 0.40 | |
| 95LVC-10A | rhyolite tuff | bio | | | 53.13 | 0.49 | 0.49 | 0.50 | |
| LVC-19-3 | andesite porphyry | plag | | | 53.33 | 1.93 | 1.93 | 1.93 | |
| 95LVC-7 | intrusive rhyolite porphyry | hbld | | | 53.37 | 0.24 | 0.25 | 0.26 | |
| *Anaconda Core Complex* | | | | | | | | | |
| ME-1 | mylonite below main detachment in Anaconda Range | musc | ih | FCs | 47.89 | 0.28 | 0.28 | 0.30 | O'Neill et al. (2004) |
| *Bitterroot Core Complex* | | | | | | | | | |
| B85 | Whistling Pig pluton | kspar | iso | Mmhb | 48.38 | 0.61 | 0.61 | 0.61 | House et al. (2002) |
| B85 | " | bio | iso | | 49.19 | 0.81 | 0.81 | 0.82 | |
| EM3b | Spruce Creek mylonite zone | musc | iso | | 49.29 | 0.61 | 0.61 | 0.61 | |
| EM3c | " | bio | iso | | 49.90 | 1.01 | 1.01 | 1.02 | |
| NB12-11 | Skookum Butte stock | bio | iso | | 50.81 | 1.01 | 1.01 | 1.02 | |
| NB12-11 | " | kspar | iso | | 53.04 | 2.02 | 2.02 | 2.03 | |
| EM3b | Spruce Creek mylonite zone | kspar | iso | | 53.95 | 1.01 | 1.01 | 1.02 | |
| EM3d | " | bio | iso | | 54.45 | 2.02 | 2.02 | 2.03 | |
| EM6 | " | bio | iso | | 54.86 | 0.61 | 0.61 | 0.61 | |
| EM3d | " | hbld | iso | | 56.28 | 2.13 | 2.13 | 2.13 | |

*Notes:* san-sanidine, bio-biotite, hbld-hornblende, amph-amphibole, musc-muscovite, gm-groundmass, plag-plagioclase, feld-feldspar, ih-plateau age from incremental heating experiment, dih-discordant plateau age from incremental heating experiment, iso-inverse isochron from incremental heating experiment, fus-fusion age, combo-combined fusion and incremental heating age, TCs-Taylor Creek Rhyolite sanidine, FCs-Fish Canyon Tuff sanidine, Mmhb-McClue Mountain hornblende.

*All ages have been converted to the astronomically-calibrated 28.201 Ma age for FCs of Kuiper et al. (2008) using R values and uncertainties of Renne et al. (1998).

†Analytical uncertainty

‡Analytical and intercalibration uncertainty

§Fully propagated uncertainty, calculated using equations in Kuiper et al. (2008)

TABLE DR5. RECALIBRATED $^{40}Ar/^{39}Ar$ AGES FOR EARLY AND MIDDLE EOCENE NORTH AMERICAN LAND-MAMMAL AGES

| Basin | Formation or Member | Dated unit | Age (Ma) ± 2σ* | Radioisotopic references | Biostratigraphy (zone) |
|---|---|---|---|---|---|
| Bighorn | Willwood Formation | Willwood ash | 52.90 ± 0.18 | Smith et al. (2004) | transition: Wa-6 to Wa-7 |
| Wind River | Wind River Formation | Halfway Draw tuff | 52.06 ± 0.17 | Smith et al. (2008) | Wa-7 |
| Piceance Creek | basal Parachute Creek Member | Yellow tuff | 51.55 ± 0.54 | Smith et al. (2008) | overlies Wa-7 strata |
| Fossil | Fossil Butte Member | K-spar tuff | 51.97 ± 0.16 | Smith et al. (2008) | Wa-7 |
| Greater Green River | Tipton Member | Scheggs tuff | 52.21 ± 0.16 | Smith et al. (2008) | overlies and underlies Wa-7 strata |
| | Wilkins Peak Member | Firehole, Boar, Grey, Main, Layered, and Sixth tuff beds | oldest 51.40 ± 0.25 youngest 49.92 ± 0.17 | this study, Smith et al. (2003, 2006, 2008) | laterally equivalent toWa-7, Br-0, and Br-1a strata |
| | Bridger Formation | Continental tuff | 48.96 ± 0.31 | Smith et al. (2008) | overlies Br-1b strata |
| | Bridger Formation (Bridger B) | Church Buttes & Leavitt Creek tuff beds | 49.05 ± 0.16 48.92 ± 0.31 | Smith et al. (2008) | Br-2 |
| | Laney Member | Analcite tuff | 49.24 ± 0.18 | Smith et al. (2003, 2008) | underlies Br-3 |
| | Bridger Formation (top of Bridger C) | Henrys Fork tuff | 48.44 ± 0.15 | Smith et al. (2008) | Br-3 |
| | Bridger Formation | Tabernacle Butte tuff | 48.40 ± 0.15 | Smith et al. (2008) | Br-3 |
| | Turtle Bluffs Member (Bridger E) | Sage Creek Mountain pumice bed | 47.45 ± 0.15 | Smith et al. (2008) | Ui-1 |
| Uinta–Piceance Creek | basal Upper Member (UB) and Parachute Creek Member (PCB) | Curly tuff | 49.32 ± 0.33 | Smith et al. (2008) | overlies Br-2 |
| Fowkes | Bulldog Hollow Member–Fowkes Formation | Sage ash | 48.23 ± 0.22 | Smith et al. (2008) | Br-3 |
| Wind River | Wagon Bed Formation–Unit 3 | White Lignitic tuff | 47.99 ± 0.17 | Smith et al. (2008) | underlies Ui-2 |
| Uinta | Upper Member | Blind Canyon tuff | 47.32 ± 0.22 | Smith et al. (2008) | underlies Ui-2 |
| Trans-Pecos Texas | Devils Graveyard Formation | tuff below Alamo Creek basalt | 46.85 ± 0.14 | C. Swisher in Prothero and Emry (1996) | Ui-1 |
| San Diego California | Mission Valley Formation | ash bed | 43.35 ± 0.49 | C. Swisher in Prothero and Emry (1996) | Ui-3 |
| Absaroka Volcanic Province | Trout Peak Trachyandesite | groundmass from lava flows | oldest 49.08 ± 0.14 youngest 48.69 ± 0.14 | Feeley and Cosca (2003) | overlies Br-2 |
| | Blue Point Marker | Blue Point ash | 48.41 ± 0.17 | Hiza (1999) | Br-3, underlies Ui-1 |

*Note:* See Table 3 of Smith et al. (2008) for complete references to the biostratigraphic position of dated horizons.
*Fully propagated 2σ uncertainties relative to 28.201 Ma for FCs (Kuiper et al., 2008) and R values of Renne et al. (1998).

TABLE DR6. RECALIBRATED $^{40}Ar/^{39}Ar$ AGES FOR GPTS CALIBRATION POINTS

| Dated unit | Formation or Member | Age (Ma) ± 2σ* | Radioisotopic references | Magnetostratigraphy | Magnetostratigraphy references |
|---|---|---|---|---|---|
| Willwood ash | Willwood Formation | 52.90 ± 0.18 | Wing et al. (1991); Smith et al. (2004) | C24n (base of lowest subchron) | Clyde et al. (1994); Tauxe et al. (1994) |
| Layered tuff | Wilkins Peak Member | 50.11 ± 0.16 | Smith et al. (2006) | C23n-C22r transition | Clyde et al. (1997; 2001) |
| Sixth tuff | Wilkins Peak Member | 49.92 ± 0.17 | Machlus et al. (2004) Smith et al. (2006; 2008) | C23n-C22r transition | Clyde et al. (1997; 2001) |
| Continental tuff | Bridger Formation | 48.96 ± 0.31 | this study | C22n | Clyde et al. (2001) |
| Blue Point Marker ash | overlies Aycross Formation and Trout Peak Trachyandesite | 48.41 ± 0.17 | Hiza (1999) | base of C21r | Eaton (1982); Lee and Shive (1983); Sundell et al. (1984); Flynn (1986) |
| Montenari ash | ? | 46.24 ± 0.13 | Berggren et al. (1995) | C21n | Berggren et al. (1995) |
| Mission Valley ash | Mission Valley Formation | 43.35 ± 0.49 | Prothero and Emry (1996) | C20n | Walsh et al. (1996) |

*Note:* cf. Fig. 9 of Smith et al. (2008) for chart showing relationships between magnetostratigraphic sections and $^{40}Ar/^{39}Ar$ dated horizons.
*Fully propagated uncertainties relative to 28.201 Ma for FCs (Kuiper et al., 2008) using R values of Renne et al. (1998).

TABLE DR7. RECALIBRATED AGES FOR PALEOMAGNETIC CHRONS 24N THROUGH 19R

| | Interpolated chron ages (Ma) | | | |
|---|---|---|---|---|
| Chron (base) | Cande and Kent (1992, 1995) | GTS - Ogg and Smith (2004) | Smith et al. (2008) | this study* |
| C24n.3n | 53.35 | 53.81 | 53.44 | 53.76 |
| C24n.2r | 52.90 | 53.29 | 52.89 | 53.21 |
| C24n.2n | 52.80 | 53.17 | 52.75 | 53.07 |
| C24n.1r | 52.76 | 53.12 | 52.71 | 53.03 |
| C24n.1n | 52.66 | 53.00 | 52.59 | 52.91 |
| C23r | 52.36 | 52.65 | 52.23 | 52.54 |
| C23n.2n | 51.74 | 51.90 | 50.50 | 50.80 |
| C23n.1r | 51.05 | 51.06 | 50.04 | 50.34 |
| C23n.1n | 50.95 | 50.93 | 49.88 | 50.18 |
| C22r | 50.78 | 50.73 | 49.71 | 50.01 |
| C22n | 49.71 | 49.43 | 49.07 | 49.37 |
| C21r | 49.04 | 48.60 | 48.30 | 48.59 |
| C21n | 47.91 | 47.24 | 46.52 | 46.80 |
| C20r | 46.26 | 45.35 | 45.71 | 45.99 |
| C20n | 43.79 | 42.77 | 43.16 | 43.42 |
| C19r | 42.54 | 41.59 | 42.12 | 42.37 |

*Note:* Fully propagated 2$\sigma$ uncertainties for the $^{40}Ar/^{39}Ar$ ages used as calibration points for the Eocene geomagnetic polarity timescale range from ± 0.13 to ± 0.49 m.y., and average 0.2 m.y. (cf. Table DR6). Because radioisotopic age uncertainty does not take into account stratigraphic uncertainties or uncertainty arising from interpolation of chron ages between calibration points, radioisotopic uncertainties represent the *minimum* overall uncertainty in the interpolated ages of magnetic chrons.

*Ages relative to 28.201 Ma for FCs (Kuiper et al., 2008)

**Figure Captions**

**Figure DR1.** Map showing Greater Green River Basin, sampled ash beds, and possible source regions (see Fig. DR1) and diagram showing common Pb isotopic composition of sanidine from the Analcite and Firehole tuff beds in reference to the two most likely magmatic sources for these ash beds. Common Pb isotopic compositions for the Absaroka Volcanic Province from Peterman et al. (1970), Meen and Eggler (1987), and Hiza (1999); isotopic compositions for Challis volcanics are from Norman and Leeman (1989) and Norman and Mertzman (1991).

**Figure DR2.** Stratigraphic correlation of the Wilkins Peak Member in the Union Pacific El Paso 44-3 (Roehler, 1991c), ERDA Blacks Fork no. 1 (Roehler, 1991a), and U.S. DOE Currant Creek Ridge CCR-1 (Roehler, 1991b) boreholes.

**Figure DR3.** Concordia diagrams of analyses of zircon from the Analcite and Firehole ash beds and $^{206}Pb$-$^{238}U$ age spectra diagram for 5-step CA-TIMS dissolution experiment on Analcite ash zircons. Insets are cathodoluminescence images of representative zircon crystals from each bed showing oscillatory magmatic zoning; white bars indicate 50 μm. Ellipses and weighted mean ages shown with 2σ analytical uncertainties.

**Figure DR4.** Diagrams showing age versus radiogenic $^{40}Ar^*$, analyses of Analcite and Firehole ash bed sanidine yielding < 96% are positively correlated to younger ages, interpreted to reflect the presence of authigenic orthoclase overgrowths were unremoved by air abrasion (see text).

**Figure DR5.** Chart showing age stratigraphic relationships between radioisotopic ages (all with full uncertainties), the GRF, local and global paleoclimatologic indicators (Wilf, 2000; Zachos et al., 2001), the geomagnetic polarity timescale (GPTS; c.f. Tables DR6 and DR7), and computed orbital parameters (Laskar et al., 2004). All $^{40}Ar/^{39}Ar$ ages have been converted to the 28.201 Ma age for the FCs neutron fluence standard. Numbered long eccentricity cycles for the Eocene are based on astronomical correlation "Option 2" of Westerhold et al. (2008), which gives 65.68 Ma and 55.93 Ma ages for the K/P and P/E boundaries, respectively.

**References Cited**

Berggren, W.A., Kent, D.V., Swisher, C.C., III, and Aubry, M.-P., 1995, A revised Cenozoic geochronology and chronostratigraphy, *in* Berggren, W.A., Kent, D.V., Aubry, M.-P., and Hardenbol, J., eds., Geochronology, Time Scales, and Global Stratigraphic Correlation: SEPM (Society for Sedimentary Geology) Special Publication 54, p. 129-212.

Black, L.P., Kamo, S.L., Allen, C.M., Davis, D.W., Aleinikoff, J.N., Valley, J.W., Mundil, R., Campbell, I.H., Korsch, R.J., Williams, I.S., and Foudoulis, C., 2004, Improved $^{206}Pb/^{238}U$ microprobe geochronology by the monitoring of a trace-element-related matrix effect; SHRIMP, ID-TIMS, ELA-ICP-MS and oxygen isotope documentation for a series of zircon standards: Chemical Geology, v. 205, p. 115-140.

Burnside, M.J., and Culbertson, W.C., 1979, Trona deposits in the Green River Formation, Sweetwater, Uinta, and Lincoln Counties, Wyoming: U.S. Geological Survey Open-File Report 79-737, 10 p.

Cande, S.C., and Kent, D.V., 1992, A new geomagnetic polarity timescale for the Late Cretaceous and Cenozoic: Journal of Geophysical Research, v. 100, p. 13917-13951.

—, 1995, Revised calibration of the geomagnetic polarity timescale for the Late Cretaceous and Cenozoic: Journal of Geophysical Research, v. 100, p. 6093-6095.

Clyde, W.C., Stamatakos, J., and Gingerich, P.D., 1994, Chronology of the Wasatchian Land-Mammal Age (Early Eocene): Magnetostratigraphic results from the McCullough Peaks Section. Northern Bighorn Basin, Wyoming: The Journal of Geology, v. 102, p. 367-377.

Clyde, W.C., Zonneveld, J.-P., Stamatakos, J., Gunnell, G.F., and Bartels, W.S., 1997, Magnetostratigraphy across the Wasatchian/Bridgerian NALMA boundary (early to middle Eocene) in the western Green River Basin, Wyoming: The Journal of Geology, v. 105, p. 657-669.

Clyde, W.C., Sheldon, N.D., Koch, P.L., Gunnell, G.F., and Bartels, W.S., 2001, Linking the Wasatchian/ Bridgerian boundary to the Cenozoic global climate optimum: new magnetostratigraphic and isotopic results from South Pass, Wyoming: Palaeogeography, Palaeoclimatology, Palaeoecology, v. 167, p. 175-199.

Constenius, K.N., Esser, R.P., and Layer, P.W., 2003, Extensional collapse of the Charleston-Nebo salient and its relationship to space-time variations in Cordilleran orogenic belt tectonism and continental stratigraphy, *in* Raynolds, R.G., and Flores, R.M., eds., Cenozoic Systems of the Rocky Mountain Region: Rocky Mountain Section, SEPM (Society for Sedimentary Geology): Denver, Colorado, p. 303-353.

Culbertson, W.C., 1961, Stratigraphy of the Wilkins Peak Member of the Green River Formation, Firehole Basin quadrangle, Wyoming: U.S. Geological Survey Professional Paper 424-D, p. 170-173

Eaton, J.G., 1982, Paleontology and correlation of Eocene volcanic rocks in the Carter Mountain area, Park County, southeastern Absaroka Range, Wyoming: University of Wyoming Contributions to Geology, v. 21, p. 153-194.

Feeley, T.C., Cosca, M.A., and Lindsay, C.R., 2002, Petrogenesis and implications of calc-alkanine cryptic hybrid magmas from Washburn Volcano, Absaroka Volcanic Province, USA: Journal of Petrology, v. 43, p. 663-703.

Feeley, T.C., and Cosca, M.A., 2003, Time vs. composition trends of magmatism at Sunlight volcano, Absaroka Volcanic Province, Wyoming: Geological Society of America Bulletin, v. 115, p. 714-728.

Flynn, J.J., 1986, Correlation and geochronology of middle Eocene strata from the western United States: Palaeogeography, Palaeoclimatology, Palaeoecology, v. 55, p. 335-406.

Harlan, S.S., Snee, L.W., and Geissman, J.W., 1996, $^{40}Ar/^{39}Ar$ geochronology and paleomagnetism of Independence volcano, Absaroka Volcanic Supergroup, Beartooth Mountains, Montana: Canadian Journal of Earth Sciences, v. 33, p. 1648-1654.

Hiza, M.M., 1999, The geochemistry and geochronology of the Eocene Absaroka volcanic province, northern Wyoming and southern Montana, USA [PhD thesis]: Corvallis, Oregon State University, 243 p.

House, M.A., Bowring, S.A., and Hodges, K.V., 2002, Implications of middle Eocene epizonal plutonism for the unroofing history of the Bitterroot metamorphic core complex, Idaho-Montana: Geological Society of America Bulletin, v. 114, p. 448-461.

Ispolatov, V.O., 1997, $^{40}Ar/^{39}Ar$ geochronology of the Lowland Creek Volcanic Field and its temporal relations with other Eocene volcanic areas [M.Sc. thesis]: Norfolk, Virginia, Old Dominion University, 106 p.

Janecke, S., McIntosh, W., and Good, S., 1999, Testing models of rift basins: structure and stratigraphy of an Eocene-Oligocene supradetachment basin, Muddy Creek half graben, south-west Montana: Basin Research, v. 11, p. 143-165.

Janecke, S.U., and Snee, L.W., 1993, Timing and episodicity of middle Eocene volcanism and onset of conglomerate deposition, Idaho: The Journal of Geology, v. 101, p. 603-621.

Janecke, S.U., Hammond, B.F., Snee, L.W., and Geissman, J.W., 1997, Rapid extension in an Eocene volcanic arc: Structure and paleogeography of an intra-arc half graben in central Idaho: Geological Society of America Bulletin, v. 109, p. 253-267.

Krogh, T.E., 1973, A low-contamination method for hydrothermal decomposition of zircon and extraction of U and Pb for isotopic age determinations: Geochimica et Cosmochimica Acta, v. 37, p. 485-494.

Kuiper, K.F., Deino, A., Hilgen, F.J., Krijgsman, W., Renne, P.R., and Wijbrans, J.R., 2008, Synchronizing Rock Clocks of Earth History: Science, v. 320, p. 500-504.

Laskar, J., Robutel, P., Joutel, F., Gastineau, M., Correia, A.C.M., and Levrard, B., 2004, A long term numerical solution for the insolation quantities of the Earth.: Astronomy and Astrophysics, v. 428, p. 261-285.

Lee, T.-Q., and Shive, P.N., 1983, Paleomagnetic study of the volcanic and volcaniclastic rocks from the southeastern Absaroka, Wyoming: Bulletin of the Institute of Earth Sciences Academia Sinica, v. 3, p. 155-172.

Ludwig, K.R., 1988, ISOPLOT for MS-DOS, a plotting and regression program for radiogenic-isotope data, for IBM-PC compatible computers, version 1.00: U.S. Geological Survey Open-File Report OF 88-557, 39 p.

—, 1991, ISOPLOT; a plotting and regression program for radiogenic-isotope data; version 2.53: U.S. Geological Survey Open-File Report OF 91-445, 39 p.

M'Gonigle, J.W., and Dalrymple, G.B., 1996, $^{40}Ar/^{39}Ar$ ages of some Challis Volcanic Group rocks and the initiation of Tertiary sedimentary basins in southwestern Montana: U.S. Geological Survey Bulletin 2132, 17 p.

Machlus, M., Hemming, S.R., Olsen, P.E., and Christie-Blick, N., 2004, Eocene calibration of geomagnetic polarity time scale reevaluated: Evidence from the Green River Formation of Wyoming: Geology, v. 32, p. 137-140.

Mattinson, J.M., 2005, Zircon U/Pb chemical abrasion (CA-TIMS) method; combined annealing and multi-step partial dissolution analysis for improved precision and accuracy of zircon ages: Chemical Geology, v. 220, p. 47-66.

Meen, J.K., and Eggler, D.H., 1987, Petrology and geochemistry of the Cretaceous Independence volcanic suite, Absaroka Mountains, Montana: Clues to the composition of the Archean sub-Montana mantle: Geological Society of America Bulletin, v. 98, p. 238-247.

Norman, M.D., and Leeman, W.P., 1989, Geochemical evolution of Cenozoic-Cretaceous magmatism and its relation to tectonic setting, southwestern Idaho, U.S.A.: Earth and Planetary Science Letters, v. 94, p. 78-96.

Norman, M.D., and Mertzman, S.A., 1991, Petrogenesis of Challis Volcanics from central and southwestern Idaho; trace element and Pb isotopic evidence: Journal of Geophysical Research, v. 96, p. 78-96.

O'Neill, J.M., Lonn, J.D., Lageson, D.R., and Kunk, M.J., 2004, Early Tertiary Anaconda metamorphic core complex, southwest Montana: Canadian Journal of Earth Sciences, v. 41, p. 63-72.

Ogg, J.G., and Smith, A.G., 2004, The geomagnetic polarity time scale, *in* Gradstein, F.M., Ogg, J.G., and Smith, A.G., eds., A Geologic Time Scale: Cambridge University Press: Cambridge, p. 63-86.

Parrish, R.R., Roddick, J.C., Loveridge, W.D., and Sullivan, R.W., 1987, Uranium-lead analytical techniques at the Geochronology Laboratory, Geological Survey of Canada, Radiogenic age and isotopic studies; Report 1: Geological Survey of Canada Paper 87-2, p. 3-7.

Peterman, Z.E., Doe, B.R., and Prostka, H.J., 1970, Lead and strontium isotopes in rocks of the Absaroka Volcanic Field, Wyoming: Contributions to Mineralogy and Petrology, v. 27, p. 121-130.

Prothero, D.R., and Emry, R.J., 1996, Summary, *in* Prothero, D.R., and Emry, R.J., eds., The Terrestrial Eocene-Oligocene Transition in North America: Cambridge University Press, p. 664-683.

Renne, P.R., Swisher, C.C., Deino, A.L., Karner, D.B., Owens, T.L., and DePaolo, D.J., 1998, Intercalibration of standards, absolute ages and uncertainties in $^{40}Ar/^{39}Ar$ dating: Chemical Geology, v. 145, p. 117-152.

Roehler, H.W., 1990, West-east stratigraphic correlations of surface and subsurface sections of the intertongued Eocene Wasatch and Green River formations, northern Green River basin, Wyoming: U.S. Geological Society Miscellaneous Field Studies Map MF-2149.

—, 1991a, Identification of oil-shale and trona beds and their geophysical log responses in the Energy Research and Development Administration Blacks Fork no. 1 corehole, Eocene Green River Formation, southwest Wyoming: U.S. Geological Survey Miscellaneous Field Studies Map MF-2158, 1 Sheet.

—, 1991b, Correlation and depositional analysis of oil shale and associated rocks in the Eocene Green River Formation, Greater Green River Basin, southwest Wyoming: U.S. Geological Survey Miscallaneous Investigations Series Map I-2226, 2 Sheets.

—, 1991c, Chart showing identification of oil-shale and trona beds and their geophysial log responses in the Union Pacific Railroad Company El Paso corehole no. 44-3, Eocene Green River Formation, southwest Wyoming: U.S. Geological Survey Miscellaneous Field Studies Map MF-2188, 1 Sheet.

Schärer, U., 1984, The effect of initial $^{230}Th$ disequilibrium on young U-Pb ages; the Makalu case, Himalaya: Earth and Planetary Science Letters, v. 67, p. 191-204.

Schmitz, M.D., and Bowring, S.A., 2001, U-Pb zircon and titanite systematics of the Fish Canyon Tuff; an assessment of high-precision U-Pb geochronology and its application to young volcanic rocks: Geochimica et Cosmochimica Acta, v. 65, p. 2571-2587.

Sheliga, C.M., 1980, Sedimentation of the Eocene Green River Formation in Sevier and Sanpete Counties, Central Utah [M.Sc. thesis]: Columbus, The Ohio State University, 166 p.

Smith, M.E., Singer, B.S., and Carroll, A.R., 2003, $^{40}Ar/^{39}Ar$ geochronology of the Eocene Green River Formation, Wyoming: Geological Society of America Bulletin, v. 115, p. 549-565.

Smith, M.E., Singer, B., and Carroll, A.R., 2004, $^{40}Ar/^{39}Ar$ geochronology of the Eocene Green River Formation, Wyoming; Reply: Geological Society of America Bulletin, v. 116, p. 253-256.

Smith, M.E., Singer, B.S., Carroll, A.R., and Fournelle, J.H., 2006, High-resolution calibration of Eocene strata: $^{40}Ar/^{39}Ar$ geochronology of biotite in the Green River Formation: Geology, v. 34, p. 393-396.

Smith, M.E., 2007, Stratigraphy, geochronology, and paleogeography of the Green River Formation: Wyoming, Colorado, and Utah: Madison, University of Wisconsin-Madison, 318 p.

Smith, M.E., Carroll, A.R., and Singer, B.S., 2008, Synoptic reconstruction of a major ancient lake system: Eocene Green River Formation, Western United States: Geological Society of America Bulletin, v. 120, p. 54-84.

Snider, L.G., and Moye, F.J., 1989, Regional stratigraphy, physical volcanology, and geochemistry of the southeastern Challis Volcanic Field: U.S. Geological Survey Open-File Report 89-639, p. 122-127

Snider, L.G., 1995, Stratigraphic framework, geochemistry, geochronology, and eruptive styles of Eocene volcanic rocks in the White Knob Mountains area, southeastern Challis Volcanic Field, central Idaho [M.Sc. thesis]: Pocatello, Idaho State University, 212 p.

Steiger, R.H., and Jäger, E., 1977, Subcommission on geochronology: Convention on the use of decay constants in geo- and cosmochronology: Earth and Planetary Science Letters, v. 36, p. 359-362.

Sundell, K.A., Shive, P.N., and Eaton, J.G., 1984, Measured sections, magnetic polarity and biostratigraphy of the Eocene Wiggins, Tepee Trail and Aycross Formations within the southeastern Absaroka Range, Wyoming: Wyoming Geological Association Earth Science Bulletin, v. 17, p. 1-48.

Surdam, R.C., and Parker, R.D., 1972, Authigenic aluminosilicate minerals in the tuffaceous rocks of the Green River Formation, Wyoming: Geological Society of America Bulletin, v. 83, p. 689-700.

Tauxe, L., Gee, J., Gallet, Y., Pick, T., and Bown, T., 1994, Magnetostratigraphy of the Willwood Formation, Bighorn Basin, Wyoming: New constraints on the location of Paleocene/ Eocene boundary: Earth and Planetary Science Letters, v. 125, p. 159-172.

Vandenburg, C.J., Janecke, S.U., and McIntosh, W.C., 1998, Three-dimensional strain produced by >50My of episodic extension, Horse Prairie Basin area, SW Montana, U.S.A.: Journal of Structural Geology, v. 20, p. 1747-1767.

Walsh, S.L., Prothero, D.R., and Lundquist, D.J., 1996, Stratigraphy and paleomagnetism of the middle Eocene Friars Formation and Poway Group, southwestern San Diego County, California, *in*

Prothero, D.R., and Emry, R.J., eds., The Terrestrial Eocene-Oligocene Transition in North America: Cambridge University Press, p. 120-154.
Westerhold, T., Rohl, U., Raffi, I., Fornaciari, E., Monechi, S., V., R., Bowles, J., and Evans, H.F., 2008, Astronomical calibration of the Paleocene time: Palaeogeography, Palaeoclimatology, Palaeoecology, v. 257, p. 377-403.
Wilf, P., 2000, Late Paleocene-early Eocene climate changes in southwestern Wyoming: Paleobotanical analysis: Geological Society of America Bulletin, v. 112, p. 292-307.
Wilson, A.B., and Elliott, J.E., 1997, Geologic maps of western and northern parts of Gallatin National Forest, south-central Montana: U.S. Geological Survey Geological Investigations Series Map I-2584, 1:126 720, 2 Sheets.
Wing, S.L., Bown, T.M., and Obradovich, J.D., 1991, Early Eocene biotic and climatic change in interior western North America: Geology, v. 19, p. 1189-1192.
Zachos, J., Pagani, M., Sloan, L., Thomas, E., and Billups, K., 2001, Trends, rhythms, and aberrations in global climate 65 Ma to present: Science, v. 292, p. 685-693.

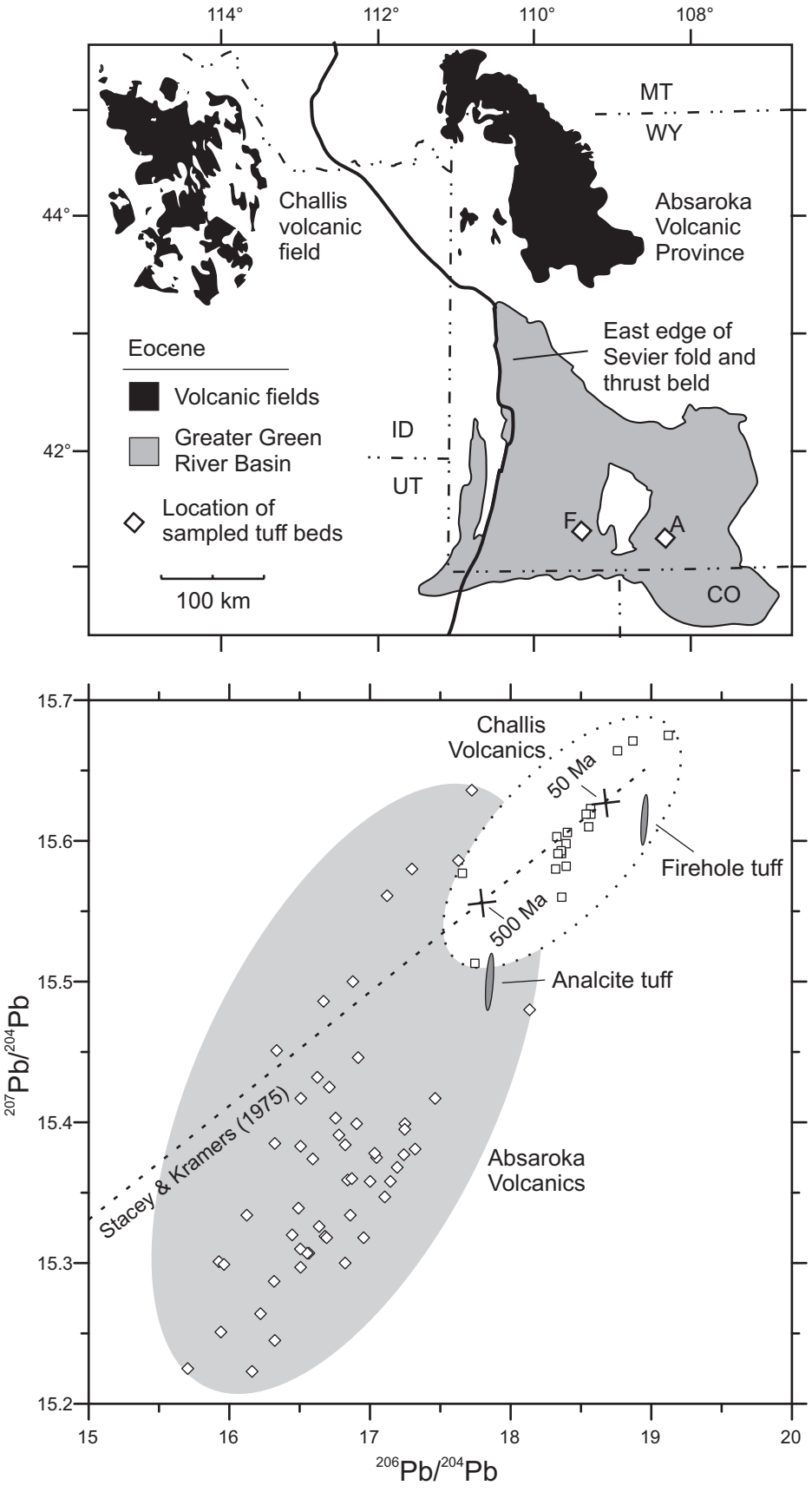
114°
112°
110°
108°
44°
42°
MT
WY
ID
UT
CO
Challis volcanic field
Absaroka Volcanic Province
East edge of Sevier fold and thrust beld
Eocene
Volcanic fields
Greater Green River Basin
Location of sampled tuff beds
100 km
F
A
15.7
15.6
15.5
15.4
15.3
15.2
15
16
17
18
19
20
$^{207}Pb/^{204}Pb$
$^{206}Pb/^{204}Pb$
Challis Volcanics
50 Ma
500 Ma
Firehole tuff
Analcite tuff
Stacey & Kramers (1975)
Absaroka Volcanics

Figure DR1

Union Pacific El Paso 44-3
US ERDA Blacks Fork no. 1
Currant Creek Ridge CCR-1
Fischer Assay gallons/ton
0
50
No core
14 km
19 km
Laney Member
Core depth (ft)
Sixth tuff
Layered tuff (Tuff No. 5)
Main tuff (Tuff No. 3)
Grey tuff
Boar tuff
Tuff No. 2
Firehole tuff (Tuff No. 1)
Rife bed
Tipton Member
Scheggs bed
I
H
G2
G1
F
E2
E1
D3
D2
D1
C
B
A2
A1
T24
T23
T22
T21
T20
T18
T17
T16
T15
T14
T13
T10
T7
T5
T2
T1
11b
11
10
9b
9a
9
8a
8
7
6
5a
5
4c
4b
4a
4
2a
2
1
500
600
700
800
900
1,000
1,100
1,200
1,300
1,400
1,500
1,600
1,700
1,800
1,900
2,000
2,100
10 m
gamma log (Roehler, 1991b)
gamma log (Roehler, 1991a)
10 meters
Key
Numbered trona beds (Burnside and Culbertson, 1979)
Siliciclastic marker beds (Culbertson, 1961)
TF6-6 Numbered oil shale beds: Burnside and Culbertson (1979)-Roehler (1991a,b)
Tuff beds numbered tuffs (Culbertson, 1961)
Numbered radioactive zones (Roehler, 1990)

Figure DR2

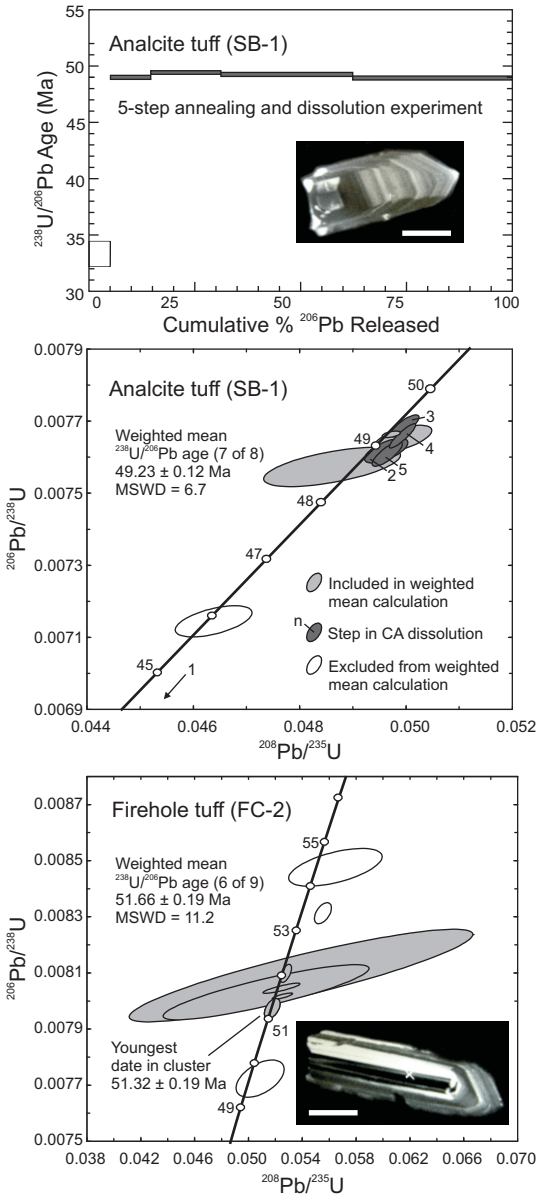
Analcite tuff (SB-1)
5-step annealing and dissolution experiment
$^{238}U/^{206}Pb$ Age (Ma)
Cumulative % $^{206}Pb$ Released
Analcite tuff (SB-1)
Weighted mean
$^{238}U/^{206}Pb$ age (7 of 8)
49.23 ± 0.12 Ma
MSWD = 6.7
Included in weighted mean calculation
Step in CA dissolution
Excluded from weighted mean calculation
$^{206}Pb/^{238}U$
$^{208}Pb/^{235}U$
Firehole tuff (FC-2)
Weighted mean
$^{238}U/^{206}Pb$ age (6 of 9)
51.66 ± 0.19 Ma
MSWD = 11.2
Youngest
date in cluster
51.32 ± 0.19 Ma
$^{206}Pb/^{238}U$
$^{208}Pb/^{235}U$

Figure DR3

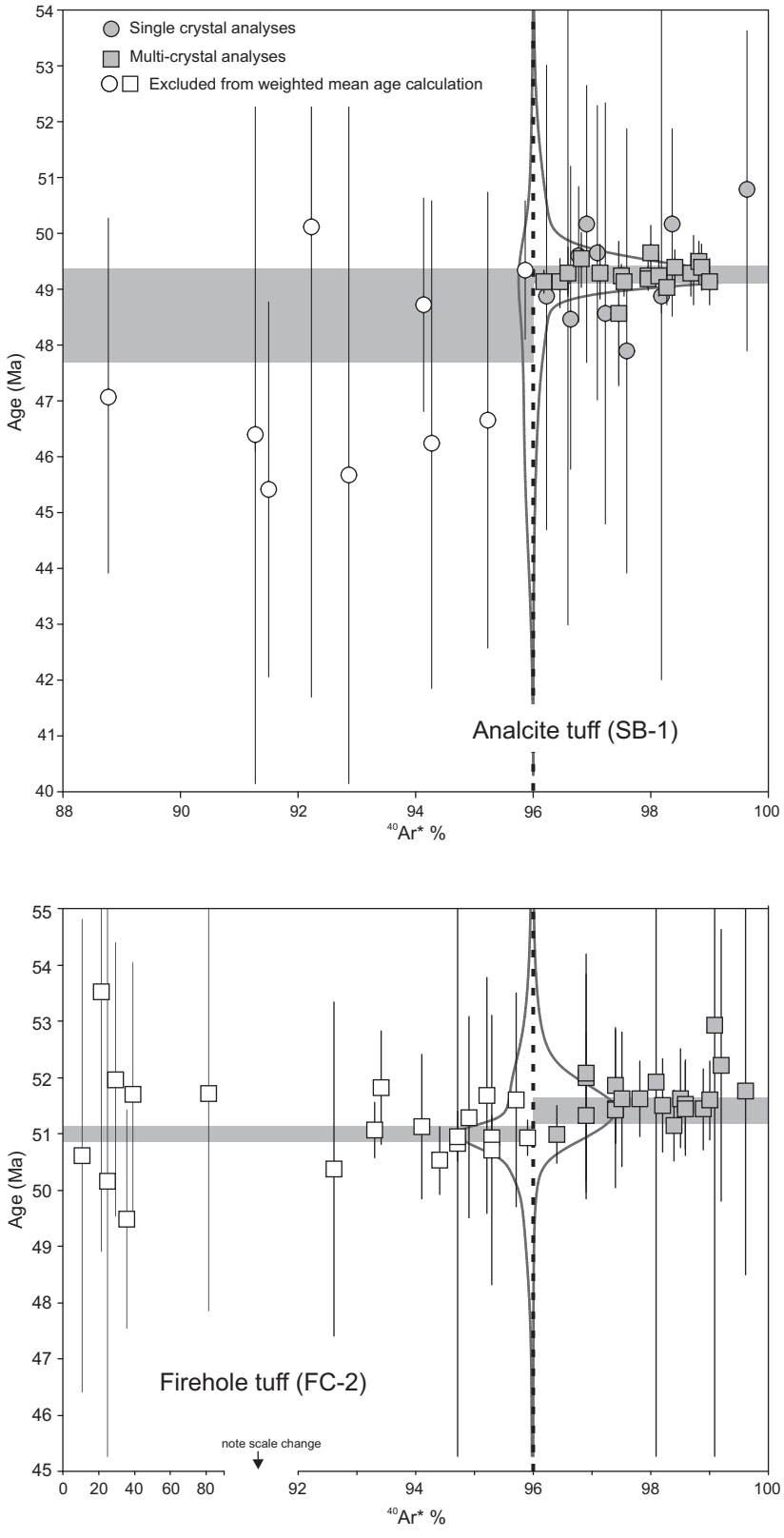
Single crystal analyses
Multi-crystal analyses
Excluded from weighted mean age calculation
Age (Ma)
$^{40}$Ar* %
Analcite tuff (SB-1)
Firehole tuff (FC-2)
note scale change

Figure DR4

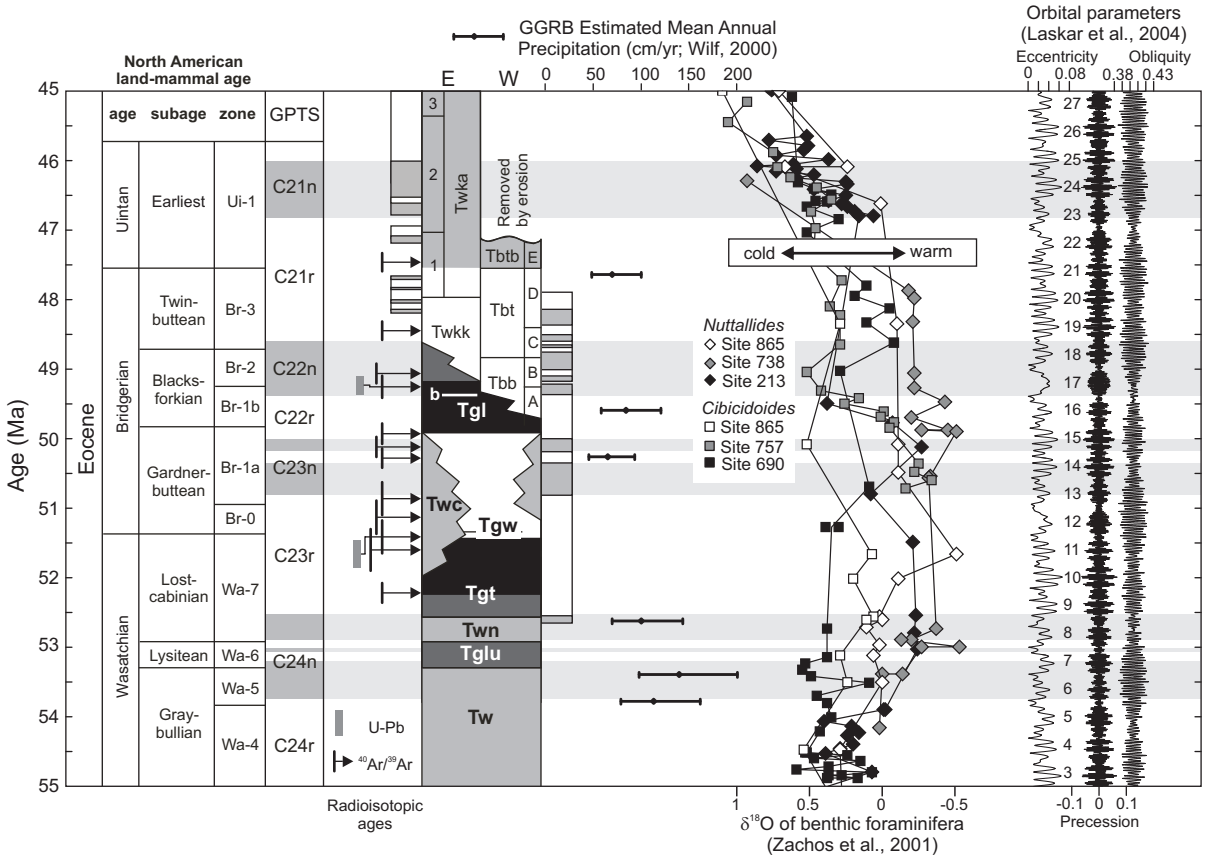
North American land-mammal age
age subage zone
GPTS
Eocene
Bridgerian
Uintan
Wasatchian
Earliest
Twin-buttean
Blacks-forkian
Gardner-buttean
Lost-cabinian
Lysitean
Gray-bullian
Ui-1
Br-3
Br-2
Br-1b
Br-1a
Br-0
Wa-7
Wa-6
Wa-5
Wa-4
C21n
C21r
C22n
C22r
C23n
C23r
C24n
C24r
Age (Ma)
GGRB Estimated Mean Annual Precipitation (cm/yr; Wilf, 2000)
E W
0 50 100 150 200
Twka
Removed by erosion
Tbtb
Tbt
Tbb
Twkk
Tgl
Twc
Tgw
Tgt
Twn
Tglu
Tw
U-Pb
40Ar/39Ar
Radioisotopic ages
cold warm
Nuttallides
Site 865
Site 738
Site 213
Cibicidoides
Site 865
Site 757
Site 690
1 0.5 0 -0.5
δ18O of benthic foraminifera (Zachos et al., 2001)
Orbital parameters (Laskar et al., 2004)
Eccentricity Obliquity
0 0.08 0.38 0.43
-0.1 0 0.1
Precession

Figure DR5